Experimental Demonstration of Modulation-Dependent Nonlinear Interference in Optical Fibre Communication

L. Galdino[(1)], G. Liga[(1)], G. Saavedra[(1)], D. Ives[(2)], R. Maher[(1)], A. Alvarado[(1)], S. Savory[(2)], R. Killey[(1)], and P. Bayvel[(1)]

(1) Optical Network Group, UCL (University College London), Torrington Place London WC1E 7JE, UK (l.galdino@ee.ucl.ac.uk)

(2) Department of Engineering, Electrical Engineering Division, University of Cambridge, Cambridge, CB3 0FA, UK

Abstract *For the first time the modulation format dependence of nonlinear interference in long-haul optical fibre transmission is experimentally demonstrated for polarisation-division multiplexed 4, 16, 64 and 256-QAM.*

Introduction

Nonlinear distortion is arguably the most important factor in limiting the performance of fibre-optic communications. Understanding the features of nonlinear interference (NLI) is critical for the design of fibre-optic communication systems and for the accurate prediction of their performance[1-6].

One of the most widely used mathematical model of NLI is the so-called Gaussian noise (GN) model[1], which is based on the assumption that the propagated signal can be modelled as a white Gaussian process, entirely specified by the power spectral density of the transmitted signal. The assumption of Gaussian signal statistics neglects most of the specific properties of the transmitted signal, including its underlying modulation format, therefore incurring a certain degree of inaccuracy in the NLI power prediction. This weakness in the model, first identified in[2] and later developed in[4] was eventually corrected and embedded as part of the original GN-model under the name of the Enhanced GN (EGN) model[5].

The EGN-model introduces an additional term to the original GN-model to account for the modulation format dependence of the NLI. That term is proportional to a specific parameter of the constellation statistical distribution: the normalised fourth-order momentum, also called excess kurtosis. The higher accuracy of the EGN-model compared to the GN-model has been demonstrated numerically[5], showing that the NLI is significantly dependent on the modulation format. However, such modulation format dependency has been demonstrated experimentally only for the case of PDM-QPSK signals[6].

In this paper, for the first time, we experimentally demonstrate the modulation format dependence of the NLI for higher constellations, comparing the NLI of PDM-*m*QAM signals, where $m \in \{4, 16, 64, 256\}$. The SNR is used as a figure of merit to estimate the NLI power variation across different PDM-*m*QAM formats. The theoretical prediction given by the EGN-model is also calculated and used as a reference for the system under investigation.

Evaluation of NLI

In an experimental scenario, the nonlinear interference power (P_{NLI}) cannot be directly measured due to the different noise components adding at the receiver. However, an indirect estimation can be performed by measuring the received signal-to-noise ratio (SNR)[1].

The total received SNR (herein SNR_{TOT}) includes different uncorrelated noise and distortion components. Each component contributes to SNR_{TOT} as in[7]

$$1/SNR_{TOT} = 1/SNR_{TX} + 1/SNR_{ASE} + 1/SNR_{NLI} \quad (1)$$

where SNR_{TX} is the transceiver limited SNR, accounting only for the transceiver noise components, whereas

$$SNR_{ASE} = P_{TX}/P_{ASE} \quad (2)$$

accounts for the lamplifier spontaneous emission (ASE) noise, where P_{TX} is the signal launched power and P_{ASE} is the ASE power, and

$$SNR_{NLI} = P_{TX}/P_{NLI} = P_{TX}/\eta P_{TX}^3 \quad (3)$$

accounts for the nonlinear noise components related to the fibre link, where η is the NLI coefficient[1] .

The SNR_{TX} was experientally measured in back-to-back (BTB), without ASE noise loading, and it represents the highest achievable SNR in the system. The SNR_{ASE} and, consequently, the

---

[1]The experimentally measured received total SNR is evaluated as the ratio between the variance of the transmitted symbols ($E[|X|^2]$) and the variance of the noise σ^2, where $\sigma^2 = E[|Y - X|^2]$ and Y represents the received symbols after the digital signal processing (DSP) is applied.

value of P_{ASE} for each span, was instead estimated after transmission by measuring SNR_{TOT} in the linear regime, where the SNR_{NLI} and SNR_{TX} are reasonably negligible. In contrast, the SNR_{NLI} in an experimental scenario cannot be estimated using equation (3), as η cannot be measured. Therefore, the SNR_{NLI} was instead obtained by subtracting the SNR_{TX} and SNR_{ASE} components from SNR_{TOT}, as shown in equation (1).

The EGN-model was used as a reference for the nonlinear transmission performance of the experimental system considered in this work. In order to adjust the theoretical model to the experimental results on the SNR_{TOT}, the SNR_{TX} and the SNR_{ASE} component were added to the SNR_{NLI}, as shown in equation (1). The SNR_{NLI} predicted from the model was calculated as described in equation (3).. The η was calculated based on the EGN-model using the nominal fibre parameters described in the next section.

Experimental transmission setup

The experimental setup is illustrated in Fig. 1. The transmitter setup is the same as described in[8]. The multi-level drive signals required for *m*QAM constellations, were generated and digitally filtered offline. The transmitted signal was a superchannel with 15 sub-channels quasi-Nyquist-spaced 8 GBd PDM-*m*QAM.

For the BTB analysis, the signal was passed directly to the coherent receiver. For transmission experiments, the output of the polarization multiplexing stage (Pol. Mux) was connected to a recirculating loop, consisting of a single 50 km span of Corning® SMF®-28 ULL fibre with an attenuation of 0.165 dB/km, and dispersion of 15.45 ps/(nm•km), a bandpass filter (BPF) and two erbium doped fibre amplifier (EDFA). The received signal and an ECL laser with 1.5 kHz linewidth used as local oscilator were combined in a digital coherent receiver as described in[8]. The offline DSP was applied as in[8] and the received SNR_{TOT} was calculated after the DSP.

Results and Discussions

The measured values of SNR_{TX} were 20.29 dB, 19.31 dB, 19.08 dB, and 19 dB for 4, 16, 64 and 256 QAM, respectively. These values represent the highest achivable SNR in our system for each modulation format.

Fig. 2 illustrates the experimental mesurements (markers) and the EGN-model (full lines) theoretical prediction of total SNR_{TOT} as functions of the launched power for 4, 16, 64 and 256 QAM after transmission over 1250 km. The performance predicted by the GN-model (dashed line) is also shown to highlight its

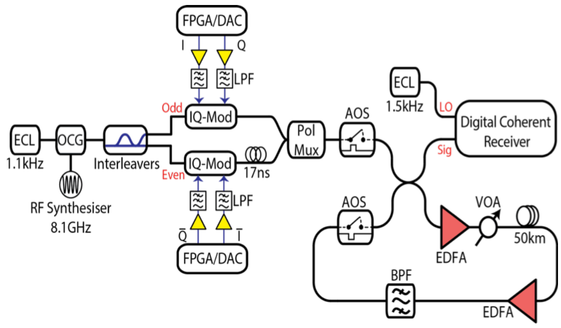

Fig. 1: Experimental setup.

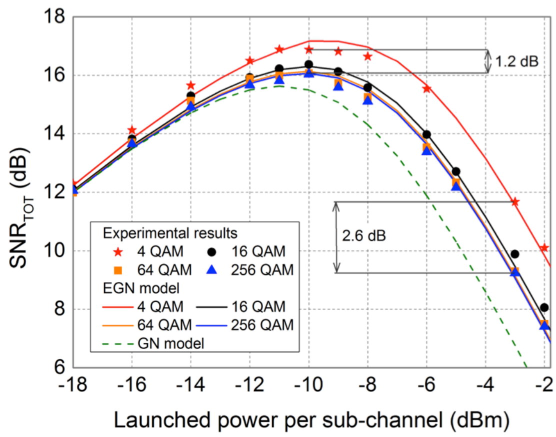

Fig. 2: Total signal-to-noise ratio as a function of the central sub-channel launched power for PDM-*m*QAM

overestimation of the NLI compared to the EGN-model predictions and the experimental measurements. As expected, in the linear regime, in which the system performance is dominated by the SNR_{ASE} component, all modulation formats converge to the same SNR_{TOT}. Conversely, at optimum launched power, at which the NLI is higher, a difference of up to 1.2 dB in SNR_{TOT} among the different modulation formats can be observed. Further increasing the transmitted powers, the system is dominated by SNR_{NLI}, and the difference in SNR_{TOT} between the different PDM-*m*QAM formats can be seen to increase towards an asympotic value. In our system, this difference is measured to be 2.6 dB between 4 QAM and 256 QAM. This diference in SNR_{TOT} in the higher nonlinear regime represents the ratio between the P_{NLI} generated by different modulation formats at a distance of 1250 km, and it is the key parameter in the characterisation of the modulation format dependence of the NLI. The GN-model prediction instead underestimates, as expected, all the measured SNR_{TOT} values in the nonlinear regime.

In order to evaluate the SNR_{TOT} accumulation over multiple spans, this parameter was measured at optimum launched power (-10 dBm) for different distances. As shown in Fig. 2, this power was sufficiently close to the optimum for all modulation formats to have negligible effect on the measurement of the maximum SNR_{TOT}, therefore allowing us to simplify the experiment without a significant loss in accuracy.

Fig. 3 illustrates SNR_{TOT} per sub-channel as a function of distance. The theoretical prediction of the EGN-model is shown using solid lines and the experimental measurements are shown using markers. At short distances, the SNR_{TOT} difference between the different modulation formats is dominated by SNR_{TX} which results in a difference in SNR_{TOT} of 1.24 dB between 4 QAM and 256 QAM after 250 km of optical fibre transmission. For longer propagation distances, where the SNR_{TOT} is dominated by the SNR_{NLI}, the difference in SNR_{TOT} among the *m*QAM signals converges to a smaller value, as expected. For instance, at 5000 km the difference in SNR_{TOT} between 4 QAM and 256 QAM is 0.85 dB, confirming the EGN-model theoretical prediction of 0.83 dB.

In order to characterise the NLI accumulation over multiple spans, Fig. 4 shows the SNR_{NLI} values (i.e. the contribution to SNR_{TOT} from the fibre nonlinear interference noise alone) at optimum launch power as a function of distance. At short distances, the difference in SNR_{NLI} among *m*QAM formats is smaller compared to that for SNR_{TOT} as shown in Fig. 3, showing the predominance of SNR_{TX} in this regime. For instance, after 250 km of optical fibre transmission, the difference in SNR_{NLI} between 4 QAM and 256 QAM is 0.97 dB (instead of SNR_{TOT} difference of 1.24 dB observed in Fig. 3). At longer transmission distances, at which the effect of SNR_{TX} become less significant, the difference in NLI converges to a value of 0.83 dB between 4 QAM and 256 QAM at 5000 km. This discrepancy is qualitatively in agreement with the EGN predictions which highlights a variation of the η coefficient over the first propagated fibre spans. The inset figure in Fig. 4 is highlighting the SNR_{NLI} for each modulation format and the GN-model prediction after 4000 km of fibre propagation. This result confirms that the different SNR performance for each modulation format studied is actually the result of the different amount the NLI generated in optical fibre transmission.

Conclusions

The properties of the signal format dependence of NLI noise in EDFA-amplified single mode fibre link without inline dispersion compensation were experimentally investigated for PDM-*m*QAM formats for the first time. As predicted by the EGN-model, the nonlinear SNR degrades with the increase of the modulation format cardinality. Also, in agreement with this model, it was shown that the NLI differences between the PDM-*m*QAM formats do not vanish as the transmission distance is increased.

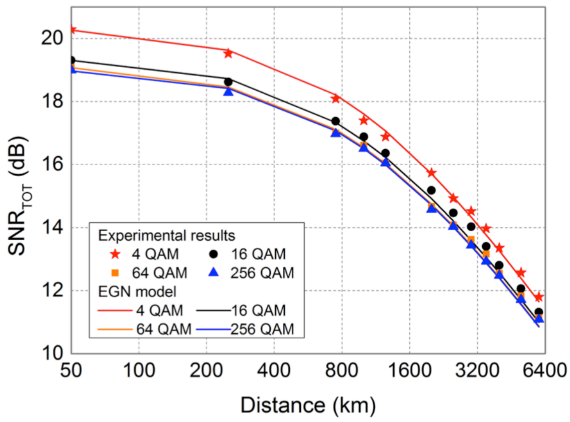

Fig. 3: Total signal-to-noise rate as a function of distance for PDM-*m*QAM constellations.

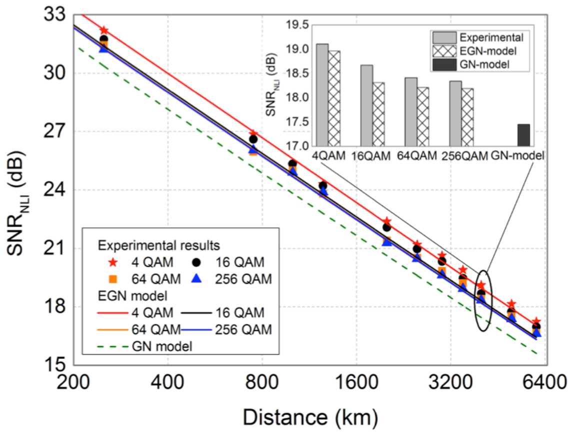

Fig. 4: Nonlinear signal-to-noise rate as a function of distance for PDM-*m*QAM constellations.

Acknowledgements

The support of UK EPSRC Programme Grant UNLOC EP/J017582/1 is acknowledgment.

References

[1] P. Poggiolini, at al., "The GN-Model of Fiber Non-Linear Propagation and its Applications," J. Light. Technol., vol. 32, no. 4, pp. 694–721, 2014.

[2] A. Mecozzi and R. J. Essiambre, "Nonlinear shannon limit in pseudolinear coherent systems," J. Light. Technol., vol. 30, no. 12, pp. 2011–2024, 2012.

[3] M. Secondini and E. Forestieri "Analytical fiber-optic channel model in the presence of cross-phase modulation," Photonics Tech. Letters, vol. 24, no. 22, 2016-2018, 2012.

[4] R. Dar, at al., "Properties of nonlinear noise in long, dispersion-uncompensated fiber links," Opt. Express, vol. 21, no. 22, pp. 25685–25699, 2013.

[5] A. Carena et al., "EGN model of non-linear fiber propagation." Opt. Express, 22, 13, 16335–62, 2014.

[6] A. Nespola, et al., "Experimental Validation of the EGN-model in uncompensated optical links," OFC, Th4D.2, 2015.

[7] F. Vacondio, et al., "On nonlinear distortions of highly dispersive optical coherent systems," Optics Express, 20, 2, 1022-32, 2012.

[8] R. Maher, el al., "Algorithms and Reach Enhancement for Ultra High Bandwidth Transceivers," OFC, Th3A.1, 2016.